DALTON
FULL PAPER

Tetrahedral d^0 and d^{10} transition metal ions sharing edges in the solid state: electronic structure and bonding

Pere Alemany,[a] Jaime Llanos[b] and Santiago Alvarez[c]

[a] *Departament de Química Física, Universitat de Barcelona, Diagonal 647, 08028 Barcelona, Spain*
[b] *Departamento de Química, Facultad de Ciencias, Universidad Católica del Norte, Avda. Angamos 0610, Casilla 1280, Antofagasta, Chile*
[c] *Departament de Química Inorgànica, Universitat de Barcelona, Diagonal 647, 08028 Barcelona, Spain*

Received 1st December 1998, Accepted 17th February 1999

The bonding and electronic structure in one- and two-dimensional copper–vanadium sulfides, based on tight binding band calculations, has been studied. Theoretical evidence for the existence of weak donor–acceptor interactions from the d^{10} copper(I) ion toward the empty d orbitals of V^V is discussed. Maximization of the number of d^{10}–d^0 interactions explains the structural choice among alternative distributions of the transition metal ions within the sulfide matrix. The double chains of $Ba_2Cu_3VS_6$ and the layers of KCu_2VS_4 have an electron deficiency associated with the presence of hypervalent sulfur bridges that slightly enhances the Cu · · · V interaction.

The metal–metal interactions between formally closed shell linear and square planar transition metal complexes have been the subject of increasing theoretical interest in recent years.[1] In particular, the linear d^{10} ML_2 and square planar d^8 ML_4 complexes give intermolecular M · · · M contacts through donor–acceptor interactions between a filled d orbital of one metal atom and the empty p orbital of another one.[2–5] Although a large number of compounds have been synthesized in which a d^{10} and a d^0 ion are put in close proximity by bridging ligands, a theoretical study of the nature of the d^{10}–d^0 interactions has not been reported so far to the best of our knowledge.

In this paper we present a semiempirical theoretical study of the electronic structure and bonding in extended structures with edge-sharing tetrahedral copper(I) and vanadium(V) ions **1**. The nature of the d^{10} · · · d^0 interactions in these compounds is not expected to be very different from that found in other molecular[6] or extended structures in which the d^{10} ion can be Cu^I, Ag^I or Au^I, and the d^0 ion Mo^{VI}, W^{VI} or V^V. The structural motif **1** can be found in tetranuclear[7] **2** or pentanuclear[8,9] complexes. A variety of other d^{10}–d^0 combinations can be found in polynuclear compounds.[6,10] Combinations of d^{10} and d^0 ions also appear forming chains[11–13] in $Ba_2Cu_3S_2VS_4$, K_2CuVS_4 and Ag_2CuVS_4, or two-dimensional networks[14–16] in KCu_2VS_4, $Na_2Cu_3VS_4$ and KCu_2NbSe_4.

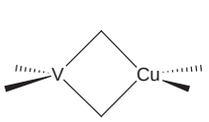

1

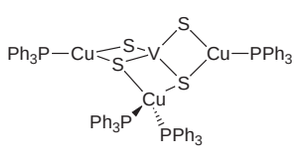

2

Bonding in the binuclear model compound $[S_2V(\mu\text{-}S)_2CuS_2]^{6-}$

As a first approximation to the electronic structure of the chains and layers of edge-sharing CuS_4 and VS_4 tetrahedra we consider the bonding in the simple molecular anion $[S_2V(\mu\text{-}S)_2CuS_2]^{6-}$, with structural motif **1**, and study the Cu · · · V interaction through an analysis of its molecular orbitals, whose energies are represented in Fig. 1. The s and p orbitals of Cu and V (not represented in Fig. 1) appear at high energy due to their strong antibonding M–S character consistent with sp^3 hybrid metal orbitals acting as acceptors toward the sulfido ligands. Among the low lying occupied levels one can identify

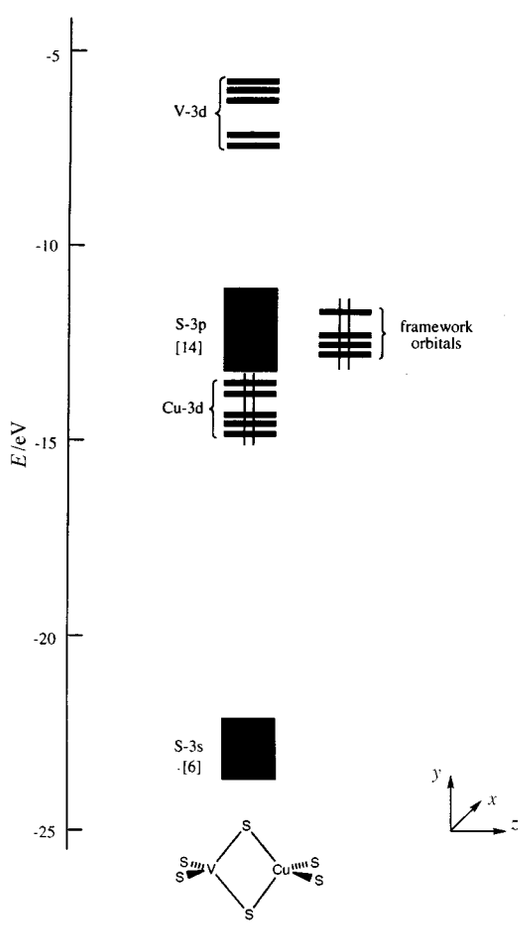

Fig. 1 Molecular orbital diagram for a model binuclear compound $[S_2V(\mu\text{-}S)_2CuS_2]^{6-}$ **1** with the structural parameters from the structure of $Ba_2Cu_3VS_6$.

the sulfur 3s and 3p orbitals, from which we single out those incorporating bonding character between the metal atoms and the bridging sulfur atoms, referred to here as *framework orbitals*. All copper 3d orbitals appear occupied at low energies, whereas empty vanadium 3d orbitals appear at high energies, in keeping with a formal description of their oxidation states as Cu^{I} and V^{V}. A small splitting of the d orbitals in t_2-like and e-like sets is also observed, as expected for an approximately tetrahedral ligand field. The splitting is inverted for the case of Cu (*i.e.*, the t_2 below the e set) because of their lower energy compared to that of the sulfur lone pair orbitals.

A small positive Cu–V overlap population (0.0046) is found in our calculations, indicative of a weak bonding interaction that could be attributed to a d^{10} to d^{0} electron donation. However, as the Cu and V atoms are held together by the bridging sulfur atoms, the positive overlap population might result from through-bond interaction. Therefore, we need to analyse the bonding relationships in the VS_2Cu ring to find out whether the positive overlap population should be attributed to the delocalized bonding in that ring or to a direct Cu–V interaction, or to both.

For an idealized structure of the binuclear compound with an M_2S_2 ring, symmetry labels corresponding to the D_{2h} point group can be used. In that case the four molecular orbitals with M–S_b bonding character (where S_b is a bridging sulfur atom) can be described schematically as in **3**. We refer to these as the framework bonding orbitals and use the symbol φ to identify them and φ* for their antibonding counterparts. Whenever these four orbitals are occupied and their antibonding counterparts empty (*i.e.* a *framework electron count*[17,18] of 8, or FEC = 8), they account for the four two-electron bonds of the M_2S_2 ring. Since one of these orbitals (a_g) is metal–metal bonding, another (b_{1u}) metal–metal antibonding across the ring, no net metal–metal bonding interaction exists when FEC = 8. However, for compounds with less electrons (FEC = 6 or 4), a short through-ring metal–metal distance would be favoured, stabilizing the occupied a_g and destabilizing the empty b_{1u} orbital. The outcome in that case is a net metal–metal bonding interaction.[17,18] Therefore, when analysing the possible existence of a bonding Cu···V interaction in the compounds under study, the possibility of electron deficiency cannot be disregarded. For that reason we have explicitly included in the MO diagram (Fig. 1) the framework orbitals **3**.

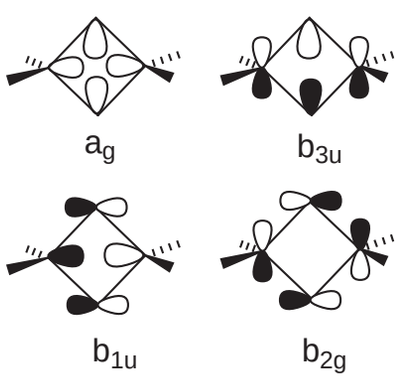

3

In our model heterobinuclear compound all the framework bonding orbitals are occupied (FEC = 8), hence no significant V···Cu bonding can be expected to arise from the framework interactions. Such qualitative reasoning is confirmed by an analysis of the contribution of each MO to the V–Cu overlap population. The largest contribution comes from the two bonding MOs composed mainly of the copper and vanadium d_{z^2} and d_{xz} orbitals, not from the framework bonding orbitals. Furthermore, if either the copper or the vanadium 3d orbitals are removed from the basis set, the V–Cu overlap

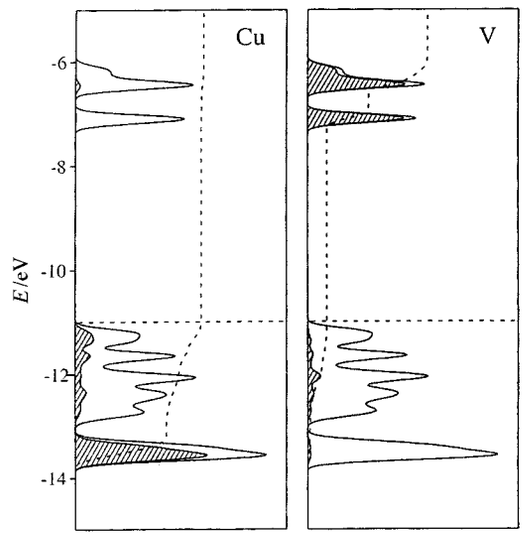

Fig. 2 Density of states (DOS) diagram around the Fermi level (horizontal dashed line) for the $CuVS_4^{2-}$ chain in K_2CuVS_4, calculated with the experimental structural data. The shaded areas represent the contribution of the Cu (left) and V atoms (right) to the total DOS. The integral of such contributions is also represented (vertical dashed lines).

population becomes negative. In summary, the weak V–Cu bonding interaction results from donor–acceptor interactions between the occupied d orbitals of Cu and the empty d orbitals of V (**4**). A small additional contribution to V–Cu bonding comes from the b_{1u} framework bonding orbital, which appears to be slightly metal–metal bonding due to mixing of the empty d orbitals (**5**, allowed by the low symmetry of the Cu–V system **1**) while a large part of its metal–sulfur bonding character is preserved. This behaviour differs from that previously found for similar interactions between two copper(I) ions, in which only copper sp^3 hybrids participate in the b_{1u} framework orbital that has the through-ring antibonding character depicted in **3**.

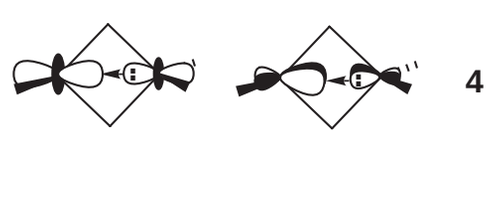

4

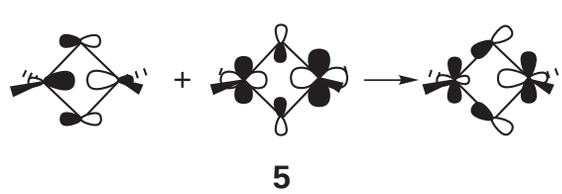

5

Electronic structure and bonding in the chain compound K_2CuVS_4

We look now at the single chains found in the crystal structure[12] of K_2CuVS_4, which can be derived by fusing together $[S_2V(\mu\text{-}S)_2CuS_2]^{6-}$ anions. The calculated density of states (DOS) diagram nicely reproduces the level ordering found for the model binuclear compound. In Fig. 2 we show the DOS in the energy window that contains the copper 3d bands (between −13 and −14 eV), the sulfur 3p bands, including the framework bonding orbitals (around −12 eV), and the empty vanadium 3d bands (above −8 eV). Other than the formation of electronic bands, no important changes appear in the

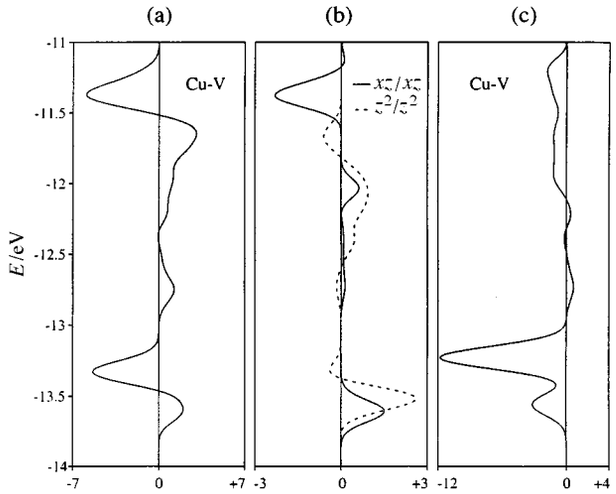

Fig. 3 Crystal orbital overlap population (COOP) curve in the region of the framework antibonding orbitals for V···Cu contacts (a) and its σ and π orbital components (b), calculated for the $CuVS_4^{2-}$ chain in K_2CuVS_4 using the experimental structural data. Also shown is the COOP curve for the V···Cu contacts calculated without the vanadium 3d orbitals (c). The scale for each COOP curve ($\times 10^2$) is indicated at the bottom.

electronic structure when moving from the binuclear to the one-dimensional compound. Again, a small positive overlap population (0.0059) is found for each Cu···V contact. If calculations are performed for the same chain but replacing the vanadium atoms by copper, a negative Cu···Cu overlap population is found, confirming that the positive Cu···V overlap population should be attributed to a weak d^{10}–d^0 donor–acceptor interaction.

A corollary of the additional stability gained by the chain through the Cu···V interactions is that the preferred structure of K_2CuVS_4 should be the one with the maximum number of Cu···V contacts. To confirm this, we repeated the calculations for an idealized chain (all M–S distances 2.30 Å) with different distributions of the metal atoms. The case in which two neighbouring Cu atoms are followed by two V atoms in the unit cell (*i.e.* ···CuCuVVCuCuV···) is found to be significantly less stable (10 kcal mol^{-1} per formula unit) than the regular chain with alternating Cu and V atoms (···CuVCuVCu···) experimentally found in K_2CuVS_4. It is thus clear that replacing Cu···Cu or V···V contacts by Cu···V ones enhances the stability of the chain.

As in the model binuclear compound studied above, the anionic chains in K_2CuVS_4 are electron precise, in the sense that all the M–S linkages can be described as two-electron bonds. This means that the electron count for each VS_2Cu ring (FEC = 8) precludes a significant degree of Cu···V bonding attributable to interaction through the bridges. This can be verified by looking at the COOP curves (Crystal Orbital Overlap Population,[19] Fig. 3). There, the Cu–V bonding peak at approximately −13.7 eV [Fig. 3(a)] coincides with bonding d_{z^2}(Cu)–d_{z^2}(V) and d_{xz}(Cu)–d_{xz}(V) peaks [Fig. 3(b)]. The bonding peak at −12.7 eV corresponds to the a_g framework orbital **3**, compensated by the antibonding peak of b_{1u} at −11.4 eV. The d_{z^2} metal orbitals interact both through space, as indicated by the bonding peak corresponding to the d_{z^2}(Cu) band (−13.7 eV), and through the bonds, as seen in the bonding region coincident with the framework bonding orbitals (around −12 eV). Furthermore, omitting the vanadium 3d orbitals from the basis set yields a COOP curve [Fig. 3(c)] in which the bonding characteristics of the copper d_{z^2} and d_{xz} orbitals have been annihilated, thus supporting the existence of a bonding donor–acceptor interaction between the d orbitals of the two metal atoms.

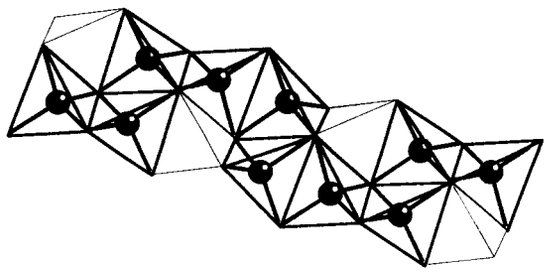

Fig. 4 Structure of the $Cu_3VS_6^{4-}$ double chain in $Ba_2Cu_3VS_6$. The tetrahedra represent the co-ordination sphere of the V atoms, the spheres represent the Cu atoms.

Electronic structure and bonding in the double chains of $Ba_2Cu_3VS_6$

Another one-dimensional compound with edge-sharing vanadium and copper ions is $Ba_2Cu_3VS_6$, which features double chains shown in Fig. 4, with an ordered distribution of vanadium and copper ions that we schematically represent for the subsequent discussion in **6a**. Notice that in such chains there are two different types of sulfur atoms. Those in the centre of the chain, labelled S_c, act as bridges to four metal atoms (μ_4 co-ordination mode) in a square-pyramidal arrangement **7**. In contrast, the external sulfur atoms, S_e, are shared by two metal atoms each, in a μ co-ordination mode.

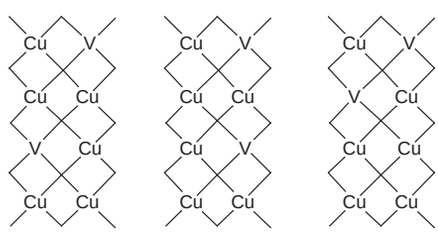

6a **6b** **6c**

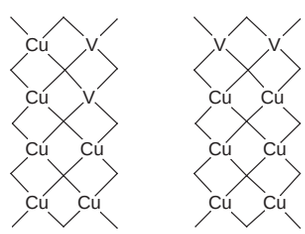

6d **6e**

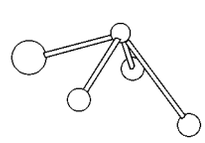

7

According to the DOS diagram (Fig. 5), the valence and conduction bands can be described from low to high energy in terms of copper 3d, sulfur 3p (including the framework bonding orbitals), and vanadium 3d orbitals. Although differences in bonding between this double chain and the single chain studied above (Fig. 3) are not apparent at first sight, a simple excercise in electron counting indicates that the double and single chains present an important difference. As already noticed, the S_c atoms present a square pyramidal environment **7**. With such geometry, one of the sulfur sp^3 lone pair orbitals is pointing away from the metal atoms, leaving only three lone pairs available to bond to four metal atoms. Since there are four S_c atoms per unit cell, each bearing one non-bonding lone-pair

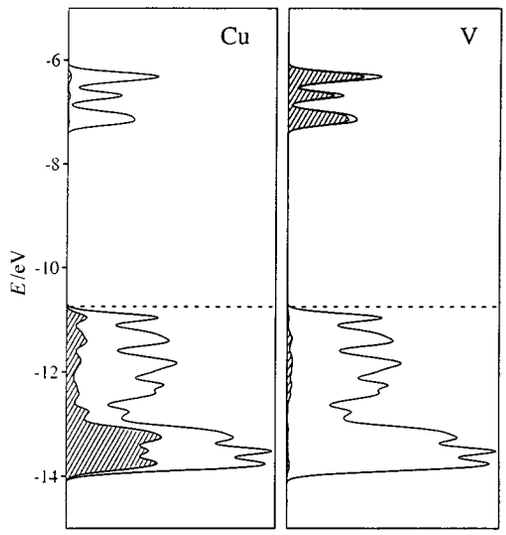

Fig. 5 The DOS diagram for the valence and conduction bands of the $Cu_3VS_6^{4-}$ double chain in $Ba_2Cu_3VS_6$, calculated with the experimental structure. The shaded areas represent the contribution of the Cu (left) and V atoms (right) to the total DOS.

orbital, and eight external S_e atoms with two outward reaching lone pairs each, there is a total of 28 sulfur valence orbitals per unit cell to construct the framework bonding orbitals (φ). But there are a total of 32 M–S linkages per unit cell, four more than the number of available electron pairs. In other words, this compound has an electron deficiency of eight electrons per unit cell with twelve metal–metal contacts. In correspondence, formally only 28 φ* orbitals can be formed, while a total of 32 4s and 4p metal orbitals are available for that. As a result, four combinations of the metal s and p orbitals are not allowed by symmetry to interact with the sulfur lone pairs. For instance, the combination of the metal 4s orbitals depicted in **8** cannot mix with the inner sulfur atoms (S_c) at the centre of the Brillouin zone.

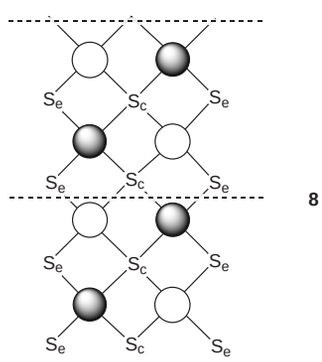

8

How is such electron deficiency reflected in the band calculations? For the analysis of the M–S bonding we have built a symmetrized $Cu_2S_3^{4-}$ double chain derived from the structure of $Cu_3VS_6^{4-}$, replacing all the V atoms by Cu. The density of states (DOS) calculated in the region of the φ* levels is presented in Fig. 6(b), together with the M–S COOP curves for the S_e and central S_c sulfur atoms. Comparison with the analogous curves for a single chain [Fig. 6(a)] shows two relevant differences: on the one hand the number of φ* bands is larger due to the doubling of the unit cell, and on the other hand there are two bands that appear at lower energy in the double than in the single chain. The lower energy of these bands is due to their non-bonding character with respect to the M–S_c bonds and little antibonding character with respect to the M–S_e bonds, as seen in the COOP curve, in contrast with the clear M–S antibonding character of all the φ* bands in the single chain. The negligible S_c contribution and the M–S_c non-bonding character of those two bands is in accord with the schematic description in **8**. On the other hand, the M–S antibonding character of these bands in the single chain implies some degree of electron transfer from the sulfur lone pairs to the metal atoms, hence partial population of metal–metal antibonding levels. In the double chain, the M–S_c non-bonding nature of the lowest two φ* bands implies a lesser population of M–M antibonding orbitals. Consequently, the bonding character of the Cu···V interaction is enhanced in the double chain (notice the higher positive value of the overlap population in the double chain compared to that in the single chain, Table 1), and even the Cu···Cu interactions become slightly bonding.

Table 1 Calculated overlap populations between the metal atoms for compounds of different dimensionalities in the experimental structures (the corresponding metal–metal distances, in Å, are given in parentheses), except for the model molecular anion $[S_2V(\mu\text{-}S)_2CuS_2]^{6-}$ for which the structure of a portion of the $[Cu_3VS_6]^{4-}$ chain was adopted

Compound	Dimensionality	Cu···V	Cu···Cu
$[S_2V(\mu\text{-}S)_2CuS_2]^{6-}$	Molecule	0.0046 (2.747)	
$[CuVS_4]^{2-}$	Single chain	0.0059 (2.719)	
$[Cu_3VS_6]^{4-}$	Double chain (parallel)	0.0128 (2.655)	0.0033 (2.732)
	(perpendicular)	0.0140 (2.737)	0.0070 (2.979)
$[Cu_2VS_4]^{-}$	Layers	0.0158 (2.704) (2.691)	−0.0033 (3.668)

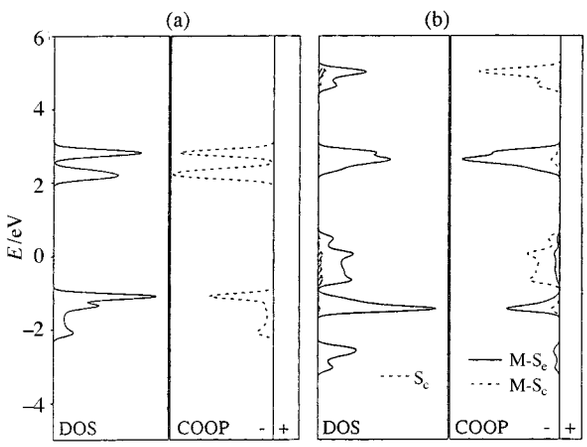

Fig. 6 The DOS diagram and COOP curve for the M–S bonds in the region of the framework antibonding orbitals, calculated for a single chain $Cu_2S_4^{6-}$ (a) and for a double chain $Cu_4S_6^{8-}$ (b). For these calculations the M–S bond distances and S–M–S bond angles were taken as 2.30 Å and 109.5°, respectively.

We must conclude that $Ba_2Cu_3VS_6$ is analogous to K_2CuVS_4 in the sense that d^{10}–d^0 bonding interactions appear in both compounds, but the electron deficiency present in the former case slightly enhances those bonding interactions. Although the asymmetry of the unit cell in the double chains of the barium salt makes a discussion of the bond distances somewhat cumbersome, the M–S_c distances are slightly longer than in the single chain of K_2CuVS_4, whereas the M–S_e ones are approximately unchanged or even slightly shorter (Table 2), as expected from the qualitative discussion above.

We turn now to the colouring problem in $Ba_2Cu_3VS_6$. In a unit cell containing six copper and two vanadium atoms several distributions of the cations can be foreseen, as sketched in **6**. With the simple qualitative idea that Cu···V, but not Cu···Cu or V···V, contacts contribute to the stability of the structure, one would easily predict that those arrangements that maximize the

Table 2 Structural data[a] for compounds of different dimensionalities with edge-sharing tetrahedra of V and M (M = Cu or Ag)

Compound	Dimensions	M–V	M–S_c	M–S_e	V–S_c	V–S_e	Ref.
K_3VS_4	0					2.053–2.163	12, 20
$TlVS_4$	0					2.171	21
$[Cu_3(PPh_3)_4VS_4]$ (**2**)	0	2.626–2.790		2.211–2.349		2.148–2.226	7
$[Cu_4(SPh)_3(dtc)VS_4]^-$	0	2.599–2.653		2.268–2.276		2.186–2.216	8
K_2CuVS_4	1	2.719		2.313		2.177	12
K_2AgVS_4	1	2.904		2.515		2.178	13
Rb_2AgVS_4	1	2.810		2.513		2.177	13
$Ba_2Cu_3S_2VS_4$	1	2.655	2.318–2.525	2.291–2.334	2.195	2.164	
		2.735[b]					11
KCu_2VS_4	2	2.692–2.704	2.298–2.300	2.292–2.300	2.233	2.146–2.192	14,22
Cu_3VS_4	3	2.697	2.299		2.219		23,24

[a] All distances in Å; S_c indicates a μ_4 atom, S_e a non-bridging, μ or μ_3 atom. [b] Connected through two μ_4 bridges.

Table 3 Relative energies (kcal mol^{-1}) and sum of all M···M and M–S (M = Cu or V) overlap populations in the unit cell for different arrangements of the metal atoms in the lattice of $Ba_2Cu_3VS_4$

Structure	Energy	M···M	M–S
6a	0.0	0.1310	10.4292
6b	−1.1	0.1344	10.4487
6c	2.4	0.1304	10.4193
6d	17.2	0.1006	10.3642
6e	17.2	0.1207	10.2583

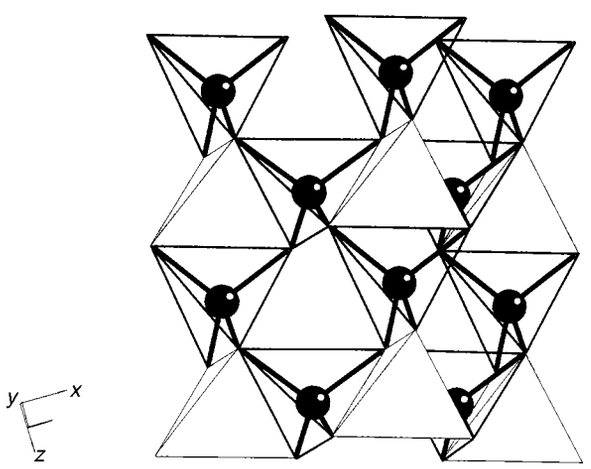

Fig. 7 Structure of the $Cu_2VS_4^-$ layers in KCu_2VS_4. The tetrahedra represent the coordination sphere of the V atoms, the spheres represent the Cu atoms.

number of Cu···V, contacts, *i.e.* **6a**–**6c** will be the most stable ones. Such qualitative expectations are supported by calculations with a symmetrized structure (Table 3). Even if one cannot fully rely on the small energy differences given by the EHTB (Extended Hückel Tight Binding) calculations on a model system with fixed geometry to predict the relative stability of structures **6a**–**6c**, it is clear that structures **6d** and **6e** should be expected to be significantly less stable. Structure **6b**, which seems a reasonable alternative to the experimental structure **6a** on energetic grounds, is likely to be less stable due to the strain introduced in a linear chain by the shorter V–S bonds compared to the Cu–S ones, a fact that has been disregarded in our model calculations by assuming identical Cu–S and V–S bond distances.

Band electronic structure of the layered compound KCu_2VS_4

The structure of KCu_2VS_4 can be described as formed by perpendicular chains of edge-sharing copper and vanadium tetrahedra (Fig. 7). The vanadium ions are connected to two Cu1 ones along the *c* axis through opposite edges, forming linear chains, and to the Cu2 ions along the *a* axis through neighbouring edges, resulting in a zigzag chain. Each Cu atom is connected to two V atoms through opposite edges of the CuS_4 tetrahedron. There are three types of sulfide ions: S2 atoms are bridging one V and one Cu1; S3 atoms are bridging one V, one Cu1 and one Cu2 atom; S1 presents an unusual umbrella-shaped co-ordination (**9**), with one V atom in the handle, two Cu2 and one Cu1 atom in the ribs. We note in passing that the same geometry is found for the sulfide ions in the three-dimensional structure of Cu_3VS_4. In what follows we will refer to the μ and μ_3 sulfur atoms (S2 and S3, respectively) as S_e, and to the μ_4 atoms (S1) as S_c.

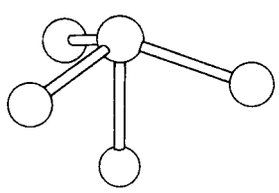

9

Again, the rule that the number of Cu···V contacts is maximized seems to apply to this compound, as would be expected if weakly attractive d^{10}–d^0 interactions exist between the two types of metal atoms. On the other hand, some degree of electron deficiency exists in this compound also. Half of the sulfur atoms in this structure (S_c) are bridging one vanadium and three copper ions in an umbrella-like fashion, thus leaving one unshared sulfur lone pair directed away from the layer. With two formula units per unit cell, two of the φ^* bands are non-bonding with respect to the umbrella sulfur atoms for a total of 24 linkages and 8 metal–metal contacts, resulting in an effective FEC of 7.5. It is interesting that in this structure all the V–S–Cu bond angles are rather small (≈73°), whereas the non-cyclic Cu–S–Cu bond angles are ≈107°. Such small angles might be taken as indication that there is an electronic preference for a short V···Cu contact, also reflected in slightly shorter Cu···V distances (2.692 and 2.704 Å) than in the single chains of K_2CuVS_4 (2.719 Å).

The DOS diagram for the valence and conduction bands of this layered compound (Fig. 8) appears to be quite similar to those of the single and double chain compounds (Figs. 2 and 5, respectively). The COOP curve for the Cu···V contacts (not shown here) presents the same features previously found for the one-dimensional chains indicating the existence of donor–acceptor interaction between the d orbitals of the two metals.

Concluding remarks

In the model molecular anion $[S_2V(\mu\text{-}S)_2CuS_2]^{6-}$ and in the single chains $[V(\mu\text{-}S)_2Cu(\mu\text{-}S)_2]_\infty^{2-}$ of K_2CuVS_4 the overlap populations and orbital analyses indicate the existence of

Table 4 Valence shell ionization potentials (H_{ii}), orbital exponents (ζ_{ij}), and combination coefficients (c_j) used for the extended Hückel calculations

Atom	Orbital	H_{ii}/eV	ζ_{ii}
S	3s	−22.761	2.122
	3p	−12.081	1.827
Cu	4s	−8.345	2.200
	4p	−4.216	2.200
	3d[a]	−13.162	5.950
V	4s	−6.850	1.300
	4p	−3.910	1.300
	3d[b]	−8.181	4.750

[a] $c_1 = 0.5933$, $\zeta_{i2} = 2.300$, $c_2 = 0.5744$. [b] $c_1 = 0.4755$, $\zeta_{i2} = 1.700$, $c_2 = 0.7050$.

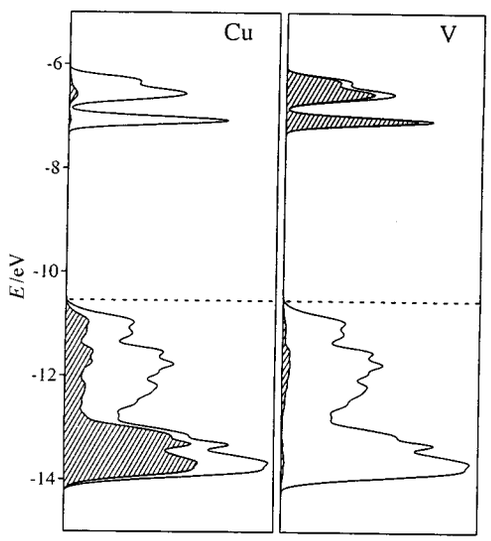

Fig. 8 The DOS diagram for the valence and conduction bands of the $Cu_3VS_6^{4-}$ layer in $Ba_2Cu_3VS_6$. The shaded areas represent the contribution of the Cu (left) and V atoms (right) to the total DOS, and the dashed line indicates the Fermi level.

weak donor-acceptor d^{10}–d^0 interactions between the Cu and V atoms. In the double chains of $Ba_2Cu_3S_2VS_4$ the d^{10}–d^0 interactions coexist with electron deficiency in the framework bonding bands that contributes to stronger Cu···V and weaker M–S interactions. *Ab initio* theoretical studies on related molecular systems with Mo^{VI} and Cu^I, Ag^I or Au^I seem to confirm the existence of weakly bonding d^{10}–d^0 interactions.[10]

An indirect evidence of the existence of stabilizing Cu···V interactions is provided by the higher calculated stability of those structures that maximize the number of Cu···V contacts, as experimentally found in the chain and layered compounds studied in this paper as well as for related extended structures with d^{10}–d^0 contacts, including compounds of different structural dimensionalities, from molecular species to the three-dimensional network of Cu_3VS_4.

Appendix

Molecular orbital and bond structure calculations presented in this work have been made with the extended Hückel method[25–27] using the modified Wolfsberg–Helmholz formula[28] for the evaluation of the off-diagonal elements of the Hamiltonian matrix. The atomic parameters adopted in these calculations are shown in Table 4. For extended systems, numerical integrations over the irreducible wedge of the Brillouin zone have been performed using a 101 k-point mesh for 1-D chains in K_2CuVS_4 and in $Ba_2Cu_3VS_6$, and a 100 k-point mesh for the layers in KCu_2VS_4.

The geometry for the binuclear model compound $CuVS_6$ discussed in the first section has been taken from the experimental structure data found for $Ba_2Cu_3VS_6$. The geometries for chains, double chains, and 2-D layers have been taken from the experimentally determined structures of K_2CuVS_4, $Ba_2Cu_3VS_6$, and KCu_2VS_4, respectively. For the analysis of the coloring problem in the chain compounds we have considered idealized structures in which all metal–sulfur distances are set to 2.3 Å and all metal atoms are supposed to have a perfect tetrahedral co-ordination environment.

Acknowledgements

Financial support to this work has been provided by Dirección General de Enseñanza Superior (Spain), project PB95-0848-C02-01 and Fonds Desarrollo Cientifico y Tecnológica (Chile), grant 1960372. S. Alvarez is grateful for a Visiting Professorship funded by Comisión Nacional de Investigación Cientifica y Tecnológica (Chile). The computing resources at the Centre de Supercomputació de Catalunya (CESCA) were funded in part through a grant by Fundació Catalana per a la Recerca and Universitat de Barcelona.

References

1 P. Pyykkö, *Chem. Rev.*, 1997, **97**, 597 and refs. therein.
2 J. J. Novoa, G. Aullón, P. Alemany and S. Alvarez, *J. Am. Chem. Soc.*, 1995, **117**, 7169.
3 G. Aullón, P. Alemany and S. Alvarez, *Inorg. Chem.*, 1996, **35**, 5061.
4 G. Aullón and S. Alvarez, *Chem. Eur. J.*, 1997, **3**, 655.
5 X.-Y. Liu, F. Mota, P. Alemany, J. J. Novoa and S. Alvarez, *Chem. Commun.*, 1998, 1149.
6 W.-W. Hou, X.-Q. Xin and S. Shi, *Coord. Chem. Rev.*, 1996, **153**, 26.
7 A. Müller, J. Schimanski and H. Bogge, *Z. Anorg. Allg. Chem.*, 1987, **544**, 107.
8 Y. Yang, Q. Liu, L. Huang, D. Wu, B. Kang and J. Lu, *Inorg. Chem.*, 1993, **32**, 5431.
9 Q. Liu, Y. Yang, L. Huang, D. Wu, B. Kang, C. Chen, Y. Deng and J. Lu, *Inorg. Chem.*, 1995, **34**, 1884.
10 F. Mota, X.-Y. Liu, C. Gimeno, A. Laguna and S. Alvarez, to be submitted.
11 C. Mujica, C. Ulloa, J. Llanos, K. Peters, E.-M. Peters and H. G. von Schnering, *J. Alloys Compds.*, 1997, **255**, 227.
12 P. Dürichen and W. Bensch, *Eur. J. Inorg. Solid State Chem.*, 1996, **33**, 309.
13 W. Bensch and P. Dürichen, *Chem. Ber.*, 1996, **129**, 1207.
14 K. Peters, E.-M. Peters, H. G. von Schnering, C. Mujica, G. Carvajal and J. Llanos, *Z. Kristallogr.*, 1996, **211**, 812.
15 C. Mujica, J. Llanos, G. Carvajal and O. Wittke, *Eur. J. Solid State Inorg. Chem.*, 1996, **33**, 987.
16 Y. Lu and J. Ibers, *J. Solid State Chem.*, 1991, **94**, 381.
17 P. Alemany and S. Alvarez, *Inorg. Chem.*, 1992, **31**, 4266.
18 G. Aullón, P. Alemany and S. Alvarez, *J. Organomet. Chem.*, 1994, **478**, 75.
19 T. Hughbanks and R. Hoffmann, *J. Am. Chem. Soc.*, 1983, **105**, 3528.
20 J. M. van den Berg and R. de Vries, *K. Ned. Akad. Wet., Ser. B: Phys. Sci.: Proc.*, 1964, **67**, 178.
21 M. Vlasse and L. Fournes, *C.R.H. Acad. Sci., Ser. C*, 1978, **287**, 47.
22 W. Bensch, P. Dürichen and C. Weilich, *Z. Kristallogr.*, 1996, **211**, 933.
23 F. E. Riedel, W. Paterno and W. Erb, *Z. Anorg. Allg. Chem.*, 1977, **437**, 127.
24 C. Mujica, G. Carvajal, J. Llanos and O. Wittke, *Z. Kristallogr.*, 1998, **213**, 12.
25 R. Hoffmann and W. N. Lipscomb, *J. Chem. Phys.*, 1962, **36**, 2179.
26 R. Hoffmann, *J. Chem. Phys.*, 1963, **39**, 1397.
27 M.-H. Whangbo, R. Hoffmann, *J. Am. Chem. Soc.*, 1978, **100**, 6093.
28 J. H. Ammeter, H.-B. Bürgi, J. C. Thibeault and R. Hoffmann, *J. Am. Chem. Soc.*, 1978, **100**, 3686.

Paper 8/09369E